

Support for the value $5/2$ for the spin glass lower critical dimension at zero magnetic field

Andrea Maiorano

*Dipartimento di Fisica, Sapienza Università di Roma, P.le Aldo Moro 2, 00185 Rome, Italy and
 Instituto de Biocomputación y Física de Sistemas Complejos (BIFI),
 Mariano Esquillor Gómez 50018 Zaragoza, Spain*

Giorgio Parisi

*Dipartimento di Fisica, Sapienza Università di Roma, P.le Aldo Moro 2, 00185 Rome, Italy and
 INFN, Sezione di Roma I, NANOTEC – CNR, P.le A. Moro 2, 00185 Rome, Italy*

We study numerically various properties of the free energy barriers in the Edwards-Anderson model of spin glasses in the low-temperature region both in three and four spatial dimensions. In particular, we investigated the dependence of height of free energy barriers on system size and on the distance between the initial and final states (i.e. the overlap distance). A related quantity is the distribution of large local fluctuations of the overlap in large three-dimensional samples at equilibrium. Our results for both quantities (barriers and large deviations) are in agreement with the prediction obtained in the framework of mean field theory. In addition, our result supports $D_{lc} = 2.5$ as the lower critical dimension of the model.

I. INTRODUCTION

Many materials undergo a phase transition at sufficiently low temperatures. It is believed that these phase transitions may be grouped into universality classes: each universality class displays its unique behavior and in the case of second order phase transitions, each class has its own critical exponents. Inside each universality class, the study of the phase transitions at space dimensions different from three is a source of inspiration for understanding how a system behaves in our three-dimensional world. Especially in the case of second order phase transitions it is very important to get a qualitative understanding of the properties of the system in the temperature-dimensions plane.

Let us consider a second order transition characterized by a disordered high-temperature phase and with an ordered low-temperature phase. Usually, there are two special values of the space dimensions D :

- The upper critical dimension (D_{uc}): the critical exponents are given by the mean field ones for space dimensions D higher than the upper critical dimension; they are non-trivial functions of the dimension D below D_{uc} .
- The lower critical dimension (D_{lc}): the low-temperature phase disappears for dimensions less than D_{lc} . In many cases, the transition temperature becomes zero when we approach D_{lc} and it is exactly zero at $D = D_{lc}$.

The lower and upper critical dimensions are universal quantities (as well as the critical exponents), in the sense that they do not depend on the microscopic details of the Hamiltonian of the system. We can check the soundness of our command of the physics of a model by trying to compute these two dimensions. Failure in doing that is a symptom we miss some crucial understanding. Indeed

ignoring the upper and/or the lower critical dimensions is actually a serious lack of understanding: in particular, ignoring the lower critical dimensions means we lack a good description of the mechanisms that lead to the disappearance of the low temperature ordered phase at low dimensions.

The success of the perturbative renormalization group techniques applied to the ferromagnetic phase transition in 3 dimensions [1], is bound to the quantitative determination of the upper critical dimension ($D_{uc} = 4$ in this case), which in turn, allowed for the quantitative control of the infrared stable fixed point and anomalous dimensions of operators in $4 - \epsilon$ dimensions and led to the ϵ expansion for the critical exponents. A similar approach is suitable for obtaining useful information starting from the knowledge of the lower critical dimension: for example in the case of spontaneous breaking of a continuous conventional symmetry (e.g. $O(N)$, $D_{lc} = 2$) one can derive a $2 + \epsilon$ expansion [2].

In the case of glassy systems, one of the theoretical difficulties is a lack of precise knowledge about the lower critical dimension: in the case of structural glasses, there is still a debate if a glass transition is present in three dimensions. The best-studied case is Ising spin glasses at zero magnetic field (i.e. the Edwards-Anderson model). The presence of a low-temperature phase in three dimensions has been proved experimentally and very large scale numerical simulations do confirm the experimental result. Franz, Parisi and Virasoro [3] (FPV) have done many years ago an analytic computation of the interface free energy between different low energy phases[36]. A byproduct of this computation is the prediction that the lower critical dimensions for spin glasses at zero magnetic field is $5/2$. This paper aims to verify numerically the correctness of the FPV formulae for the energy and the free energy of interfaces between different phases adding new evidence that the lower critical dimension is $5/2$ in

the case of Ising spin glasses at zero magnetic field. Before presenting our numerical results, we will recall the relationship between the interface free energy cost and the lower critical dimension and recapitulate some known properties of spin glasses.

A. Interfaces in ferromagnetic systems

In the case of the Ising ferromagnet ($D_{lc} = 1$) and for a Heisenberg isotropic ferromagnet ($D_{lc} = 2$), the value of the lower critical dimensions can be computed by a simple qualitative argument based on the cost of the free energy for creating an interface between two regions with different values of the order parameter. There is general consensus on impossibility of long-range order when such cost is finite in the thermodynamic limit. Sometimes the computation can be simplified by computing the increase in the ground state energy at zero temperature upon changing the boundary conditions in an appropriate way.

Let us see how to do such a computation in the Ising ferromagnet: The spins are ± 1 variables. We consider a D dimensional system, with periodic conditions in all directions x_2, \dots, x_D , but in the $x_1 \equiv x$ direction where we impose fixed boundary conditions. In the plane $x = 0$ we set $\sigma = 1$ and in the plane $x = L-1$ we set either $\sigma = 1$ (periodic boundary conditions) or $\sigma = -1$ (antiperiodic boundary conditions). Our aim is to compute the ground state energy difference as a function of L . In the case of periodic boundary conditions the ground state is all σ 's equal to 1, while in the case of antiperiodic boundary conditions the ground state is given by $\sigma(\vec{x}) = 1$ for $x_i < M$, $0 < M < L-1$ and $\sigma(\vec{x}) = -1$ for $x_i \geq M$. We immediately get the variation $\Delta E(L)$ of the energy is $2L^{D-1}$.

If we are interested in computing the free energy difference at non-zero temperature, not too near to the critical point, we can write a Landau-Ginzburg-like expression for the magnetization $m(\vec{x})$. One finds that the variation of the free energy is $\Sigma(T)L^{D-1}$, where $\Sigma(T)$ is the surface tension. The free energy increase of the free energy in $D = 1$ goes to a constant for large L and therefore $D_{lc} = 1$ is the lower critical dimensions.

In the planar spin model case spin waves are present and we can have smooth interfaces with much lower free energy cost. In this model the spins are two dimensional vectors of modulus 1 and they can be parametrized as $\sigma(\vec{x}) = \{\cos(\theta(\vec{x})), \sin(\theta(\vec{x}))\}$. Neglecting vortices, in the continuum limit the phase $\theta(\vec{x})$ is a smooth function. In the low temperature regime we can write an effective free energy as

$$AL^{D-1} \int d^D x \left(\frac{d\theta(\vec{x})}{dx} \right)^2. \quad (1)$$

where $\theta(\vec{x})$ denote the direction of the magnetization around the point \vec{x} and A is a positive constant. This

expression can be derived from a Landau Ginsburg functional (or equivalently from the Goldstone model) where one neglects the longitudinal fluctuations in the direction of the magnetizations.

In this case we can introduce more complex boundary condition: e.g. $\theta(x_1)|_{x_1=0} = 0$ and $\theta(x_1)|_{x_1=L-1} = \theta_B$. A detailed computation (see appendix A) tells us in this case we can construct an interface where the phase $\theta(\vec{x})$ is a smooth function. We find that the free energy increases as $AL^{D-2}\theta_B^2$, hence $D_{lc} = 2$. A similar results is obtained for the internal energy. Indeed in $D = 2$ these differences remain of order 1, also when $L \rightarrow \infty$.

The absence of a phase with a non-zero order parameter in two dimensional systems is the essence of the Mermin-Wagner-Hohenberg [4, 5] theorem where one studies small fluctuations around equilibrium, proving that in presence of non-zero order parameter the correlation function in the small momentum region behaves as $1/k^2$ (i.e. a Goldstone Boson is present) and this behavior is inconsistent in a 2D world.

B. Spin glasses: experimental and numerical results

A popular model of spin glasses at zero magnetic field is the *Edwards-Anderson* model [6] (EA) in which the Ising spins $\{\sigma\}$ are arranged on a D dimensional cubic lattice. Only interactions among nearest neighbors pairs contribute to the energy: the Hamiltonian is given by

$$H = - \sum_{\langle i,k \rangle} J_{i,k} \sigma_i \sigma_k, \quad (2)$$

where the $J_{i,k} = \pm 1$ are quenched (frozen) random couplings. Different realizations of the configuration of couplings $\{J\}$ define different *instances* (or *samples*) of the system. Two or more independent copies of the same instance are called *replicas*.

In the low-temperature phase a crucial quantity that plays the role of order parameter is the expectation value of the overlap $q_i \equiv \sigma_i \tau_i$, where σ_i and τ_i are spins at site i in any two independent equilibrium configurations. We define the *intensive* value of the overlap in a box of linear size L as

$$Q = \frac{1}{L^D} \sum_i q_i. \quad (3)$$

In the mean field approximation the thermal average $\langle Q^2 \rangle_J$ for a given disorder instance is non-zero below the transition temperature in the infinite volume limit. For a given sample the overlap may take many different values and with changes in the *extensive* free energy that are of order 1: in other words there are globally different arrangements of the spins that have comparable probabilities. As a consequence the overlap probability distribution function $P_J(Q)$ (see details in the appendix B)

is of order 1 for many different values of Q : $P_J(Q)$ depends on the choice of the J 's (non-self averageness); also $\langle Q^2 \rangle_J$ depends on the values of the J 's. If we take two different equilibrium configurations of the system (e.g. $\{\sigma\}$ and $\{\tau\}$) their global overlap Q can be in the range $[-q_{EA} : q_{EA}]$, where, denoting by $[\dots]_J$ the average over samples, $q_{EA} = [\langle s_i \rangle^2]_J$ is the so-called *EA order parameter*, without any additional cost. The Q -constrained free energy density $F(Q)$ is constant in this interval as shown by an explicit computation. The existence of flat regions in free energy has deep consequences.

The mean field theory is relatively well understood: it is valid in the simple Sherrington Kirkpatrick model that naively correspond to the infinite-dimensional limit of the Edwards-Anderson model. In finite dimensions, the analytic studies are more complex. Standard arguments can be used to construct a low momentum effective Landau-Ginzburg theory and apply renormalization group-like techniques [7]. The system has a standard second-order phase transition with a divergent nonlinear susceptibility $\chi^{(3)}(T) \propto (T - T_c)^{-\gamma}$. It has been shown that in dimensions greater than 6 the critical exponents are those of mean field (i.e. $\gamma = 1$). An ϵ expansion for the critical exponents has been constructed in $\epsilon = 6 - D$ [8]: the series have been computed up to the order ϵ^3 [9] but unfortunately the convergence of the series is not good and it is difficult to use them already in dimensions $D = 5$.

Quite accurate experiments [10] and numerical simulations [11] agree on the existence of a transition in dimensions $D = 3$, with quite a large value of γ (i.e. $\gamma \approx 6$), therefore $D_{lc} < 3$. On the contrary in dimensions $D = 2$ the non-linear susceptibility is finite at any positive temperature and it has a power-law divergence in the zero temperature limit. According to standard folklore, at the lower critical dimensions, the relevant susceptibility should diverge exponentially when the temperature goes to zero and a power-law divergence should be present only below the lower critical dimensions. Numerical simulations done by Boettcher [12, 13] gives $D_{lc} = 2.4986$ with a small error. Boettcher studies the exponent that controls the dependence on L of the variance of the energy difference from periodic to antiperiodic boundary conditions for different dimensions D . This exponent should change sign at the lower critical dimension: its value is obtained by interpolating (as a function of the dimensions D) this critical exponent. A similar estimate $D_{lc} = 2.491$ (not accurate as the previous one) comes from the extrapolation of the values of the critical temperature [14] as a function of dimensions, assuming that T_c vanishes proportionally to $\sqrt{D - D_{lc}}$, as suggested by theoretical considerations [15] [37].

Summarizing, numerical simulations and experiments tell us that $2 < D_{lc} < 3$. There are also strong numerical pieces of evidence that the value of D_{lc} is quite near to and likely equals $5/2$ [38].

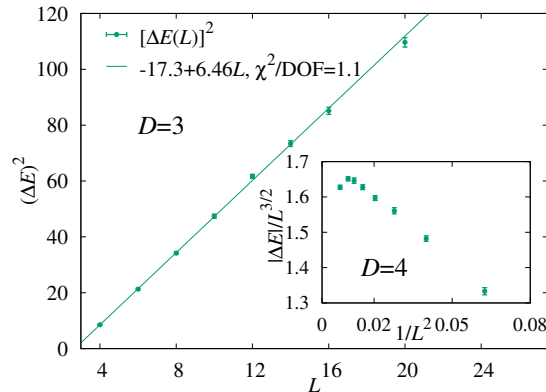


FIG. 1: Main plot, $D = 3$: $\Delta E(L)^2$ as a function of L at $T = 0.7$. The theory predicts an asymptotic linear behavior. In the inset, $D = 4$: $\Delta E(L)/L^{3/2}$ as function of $1/L^2$ at $T = 1.4$. The theory predicts a finite non zero limit at $1/L = 0$.

C. Interfaces in spin glasses

The value $D_{lc} = 5/2$ was predicted in 1993, much before Boettcher's work, in a remarkable paper [3] assuming that there are minimal corrections to mean field theory predictions[39].

We have seen that we can define a free energy as a function of the global overlap Q and the Q -constrained free energy density $F(Q)$ is constant for $|Q| < q_{EA}$. A natural question arises when we constrain two different large regions of the system to have two different values of Q . The bulk contribution to the free energy vanishes, and we remain with the contribution coming from the interface that we have to evaluate.

In the paper [3], FPV considered two systems A and B with the same Hamiltonian (i.e. same $\{J\}$) inside a D dimensional box of side L . Using the same geometry that we have discussed above, they studied the free energy increase when we constrain the two systems to have a mutual overlap Q^{AB} with a value $Q^{AB} = Q$ on a plane on the boundary at $x = 0$ and $Q^{AB} = Q' = Q + \Delta$ at the other boundary at $x = L$. The computation was done for small Δ in the region where both Q and Q' are in the range $[-q_{EA} : q_{EA}]$. We can write $q(x) = Q + \theta(x)$ with

$$\theta(0) = 0 \quad \text{and} \quad \theta(L) = \Delta. \quad (4)$$

One can thus compute the free energy cost by using a variational procedure with respect to all other variables (i.e. probability distribution of all the overlaps Q^{AA} for system A, Q^{BB} for system B and all the overlaps Q^{AB} except those on the boundary). One finally arrives at the expression for the free energy increase $\Delta F_L[\theta]$ that is a functional of $\theta(x)$. At the end of the day, we have to minimize $\Delta F_L[\theta]$.

The results of this explicit computation were rather surprising. A simple quadratic analysis of the free energy [40] implies that the final result is the sum of a few terms

of the form

$$\Delta F_L[\theta] = AL^{D-1} \int_0^L dx \left(\frac{d\theta(x)}{dx} \right)^2. \quad (5)$$

However when all the terms are assembled these quadratic contributions cancel out. No free energy increase is present if we consider only quadratic terms.

If we keep higher-order terms (e.g. the cubic terms) we get nonlinear terms in the mean field equations. Finally we obtain the amazing result:

$$\Delta F_L[\theta] \propto L^{D-1} \int_0^L dx \left(\frac{d\theta(x)}{dx} \right)^{5/2}. \quad (6)$$

This result can also be generalized to the case of a function $\theta(\vec{x})$ that depends on all the coordinates of \vec{x} .

$$\Delta F_L[\theta] \propto \int_0^L dx^D \left(\sum_{\nu=1,D} \left(\frac{\partial\theta(\vec{x})}{\partial x_\nu} \right)^2 \right)^{5/4}. \quad (7)$$

We finally obtain that the free energy increase is given by

$$\Delta F(L, \Delta) \equiv \min_{\theta} \Delta F_L[\theta] \propto L^{D-5/2} \Delta^{5/2}, \quad (8)$$

where the minimum is done over all the functions $\theta(x)$ that satisfy the boundary conditions eq. (4). A similar expression is obtained for the internal energy.

This analysis implies that the barriers are much smaller than in the known cases of spontaneous breaking of a continuous symmetry (the nature of the Goldstone modes is quite different). At the end we find that the barriers vanish for $D \leq 2.5$, hence $D_{lc} = 2.5$.

II. RESULTS AND DISCUSSION

It is clear that the validity of the FPV result, which has been derived in the mean field framework, can be considered doubtful. However, a similar result also holds in the ferromagnetic case, when other properties of mean field theory are not valid. Indeed detailed arguments show that the interaction of Goldstone Bosons (magnons in this case) is essentially the same as in mean field theory.

The FPV theory predicts a value of the lower critical dimension that is very near to the one suggested by earlier numerical simulations. In order to check its validity beyond the assumptions used for its derivation, we have investigated the agreement of its predictions with the results of purposely designed numerical simulations. As we shall see the results are in remarkable agreement.

We will consider two different kinds of simulations: the direct measurement of the interface energy and the study of large deviations of the overlap differences in the same sample at equilibrium.

A. Direct measurement of the Interface Energy

We have computed directly the interface energy $\Delta E(L, Q, \Delta)$ in $D = 3$ and $D = 4$ in the most extreme case $Q = 0$ and $\Delta = 2$, i.e. $Q = 1$ on one boundary and $Q = -1$ on the other boundary. We have studied this extreme case for two reasons: the signal to noise ratio is higher and its numerical implementation is much simpler than that in the case where $\Delta < 2$.

An FPV computation predicts that both the interface energy $\Delta E(L)$ and interface free energy $\Delta F(L)$ grow as $L^{1/2}$ for $D = 3$ and as $L^{3/2}$ for $D = 4$. We have studied only the internal energy that can be computed in a much simpler way than the free energy.

The data we will discuss below have been produced by simulations of the EA model equation 2 with binary couplings ($J_{ij} = \pm 1$ with equal probability) in $D = 3$ and $D = 4$. (see section *Methods* below for details). The critical temperature for the model is $T_c \simeq 1.103$ in $D = 3$ [16] and $T \simeq 2.0$ in $D = 4$. [17] We have done our simulations at a temperature of the order of $0.7T_c$. At this value of the temperature thermalization of the samples is not too difficult, and we are far enough from the critical temperature for simulations to be not too sensitive to crossover effects. More precisely our simulations have been done at $T = 0.7 \simeq 0.64T_c$ in $D = 3$ and at $T = 1.4 \simeq 0.7T_c$ in $D = 4$.

We report data for the square of the interface energy $\Delta E(L)^2$ as a function of the linear size up to L for both $D = 3$ (up to $L = 20$) and $D = 4$ (up to $L = 12$) in Figure 1.

A linear growth of $\Delta E(L)^2$ describes very well the $D = 3$ data, in very good agreement with the theoretical prediction that gives $\Delta E(L) \propto L^{1/2}$. A linear fit to $\Delta E(L)$ works surprisingly well also at L as small as 4 up to the largest value of L , i.e. $L = 20$. The reasons for such small finite size corrections in $D = 3$ are unclear.

In dimensions $D = 4$ data have stronger finite size corrections, but the ratio $|\Delta E(L)|/L^{3/2}$ tends to saturate at larger sizes. Unfortunately, we are limited to consider values of L up to 12 in $D = 4$ - that correspond to 20736 spins, a number already much larger than the number of spins (8000) that we used in $L = 20$ for $D = 3$.

Both three-dimensional and four-dimensional data strongly support the prediction $\Delta E(L) \propto L^{D-5/2}$.

The results we obtain for the scaling exponent of energy differences are larger than previous numerical estimates by measuring the energy cost of flipping boundary conditions in ground state computations [14, 18]. We stress we have a completely different setting here, the main difference being the imposed constraint (fixed total overlap Q and overlap difference between opposite boundaries Δ) determining completely different excitations (see discussion in the appendix D).

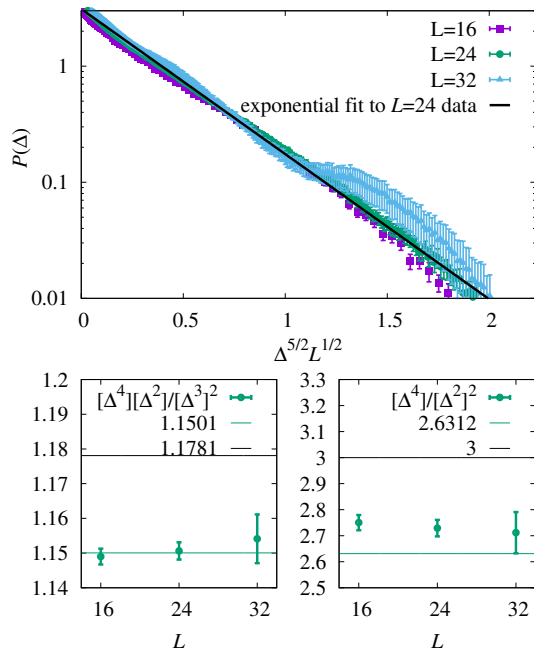


FIG. 2: Top panel: $P(\Delta_M, L)$, $M/L = 1/8$ (see text) as function of $z \equiv L^{1/2}\Delta^{5/2}$, $T \simeq 0.64T_c$. Bottom panels: Comparison of cumulants obtained from the numerical data (points with errorbars) and values obtained with the prediction equation 10 (green line) and expected for a Gaussian distribution (black line); right: the Kurtosis K ; left: the cumulant ratio R (see text).

B. Large deviations of local overlaps fluctuations in a sample

We could use the previous approach to study also the Δ dependence of the Energy barriers by performing a different simulation for each value of Δ . Here we prefer to do the direct tests of equation 8 for the *free energy*, computing the probability of rare configurations in existing large scale simulations performed by the Janus collaboration [19, 20].

In the low-temperature phase, the local overlaps $q(\vec{x})$ of two equilibrium configurations should fluctuate around the volume average of q , i.e. Q . The probability of having a rare fluctuation with an overlap value q significantly different from Q in a large region is exponentially damped and it can be computed starting from equation (6). The computation could be done by means of a standard simulation of spin glasses and looking for the probability distribution of these rare events. A computation along this baseline for hierarchical spin glass models on Dyson lattices can be found in [21]. We find convenient to use the large database of the Janus collaboration that contains already thermalized spin glass configurations for quite large lattices (up to $L = 32$ and down to $T = 0.64T_c$ in $D = 3$).

The region where we look for large fluctuations of Q may be a cube, as in the case of window overlaps, however

in this case we consider a very simple geometric setting. Let us define the quantities of interest. We work in $D = 3$ in a box of size L with periodic boundary conditions. We define the overlap $q_{M,x}$, obtained by averaging the local overlap in a region of size $L^2 \times M$ delimited by $x \leq i_x \leq x + M - 1$:

$$q_{M,x} = \frac{1}{ML^2} \sum_{x \leq i_x \leq x+M-1} \sum_{i_y, i_z} q(i_x, i_y, i_z) \quad (9)$$

We are interested in computing the probability of having $q_{M,x}$ quite different from the global average Q . In order to simplify the analysis we define $\Delta_M = \frac{1}{2}|q_{M,x} - q_{M,x+L/2}|$, i.e. the difference in the overlap of two regions of size $L^2 \times M$ that are at the largest possible distance (we are using periodic boundary conditions), normalized in $[0, 1]$

The quantity of interest is the probability density of Δ_M inside a box of size L , i.e. $P_M(\Delta_M, L)$, with fixed total overlap in the two regions $Q_M = |q_{M,x} + q_{M,x+L/2}|$, in the large deviation region where this probability is small; we consider $Q_M = 0$ (see section *Methods*) allowing for the largest range of fluctuations Δ and more statistics in the large deviation region. We average $P_M(\Delta_M, L)$ over all samples. In the large deviation region, this probability is given by the exponential of the free energy difference multiplied by $-\beta$. The prediction of FPV is

$$P_M(\Delta_M, L) \propto \exp\left(-A_{M,L}L^{1/2}\Delta_M^{5/2}\right) \quad (10)$$

in the large deviation region $z \equiv L^{1/2}\Delta_M^{5/2} \gg 1$ and Δ_M not too large. The coefficient $A_{M,L}$ does depend on the details of the free energy and therefore it cannot be computed: however, we can compute its dependence on M : as we shall see it turns out to be a function of M/L .

We plot $P_M(\Delta_M, L)$ in $D = 3$ at $T = 0.7$ as a function of $z = L^{1/2}\Delta^{5/2}$ for $L = 16, 24, 32$ and $M/L = 1/8$ in Figure 2, top panel. The $L = 32$ data at the largest z values are noisy, due to the lower statistics that we have at this value of L . The theoretical prediction $\exp(-Az)$ is accurate in almost all the range, showing deviations from an exponential decay only at very small z values: these deviations are an expected effect because at small Δ_M we must have $P_M(\Delta_M, L) = P_M(0, L) - O(\Delta_M^2)$.

We have computed the cumulant ratios

$$K = \langle \Delta^4 \rangle / \langle \Delta^2 \rangle^2, \quad R = \langle \Delta^4 \rangle \langle \Delta^2 \rangle / \langle \Delta^3 \rangle^2 \quad (11)$$

whose numerical values (depicted in Figure 2, bottom panels) compare well with the values predicted using equation 10. These are only approximate predictions because both K and R depend on the behavior of $P_M(\Delta_M, L)$ in the region of small z where the large deviation behavior $\exp(-Az)$ is not expected to hold. The ratio R has been constructed in such a way to be less dependent on the value of the probability in the small z region: its value is remarkably in better agreement with the theoretical predictions than the Kurtosis K .

We have also looked at the dependence of $A_{M,L}$ as a function of M/L . The theoretical predictions (derived in the *Methods* section) are shown in fig. 3 and are in very good agreement with the numerical data.

III. CONCLUSIONS

The numerical evidence presented above strongly support the correctness of the FPV prediction on the lower critical dimension $D_{lc} = 5/2$ and the scaling of the free energy interface barriers. It is remarkable that the corresponding exponents have a simple functional dependence on D and they do not show any of the usual anomalous corrections when extending below the upper critical dimension. This phenomenon is typical of interface energies in the broken symmetry phase where these quantities are not changed by corrections to mean field theory: it is also related to the decoupling of Goldstone type modes at low momenta. Here the situation is far more complex because the analysis is based on non-linear corrections and it does not match with perturbative corrections.

In spin glasses, one can define constrained connected correlation functions: $C(x|Q) \equiv \langle q(x)q(0) \rangle_Q - Q^2$, where the average is done in a two replica system where the total overlap is Q . Dimensional analysis implies that $C(x|Q) = B(Q)x^{-\alpha}$ with $\alpha = 4/5(D - 5/2)$ in the region of $Q < Q_{EQ}$. In $D = 3$ large lattices simulations give $\alpha(Q)$ independent from Q , equal to 0.38 ± 0.02 against the theoretical prediction of $2/5$ [22].

In momentum space the FPV prediction becomes $\tilde{C}(k|Q) \propto 1/(k^2)^{D/5+2}$. This last prediction on the momentum behavior poses more questions. An expansion around mean field [23] in high dimensions gives two different exponents α depending on the value of Q . At $Q = 0$: $\alpha(0) = D - 4$; at $0 < Q < Q_{EA}$: $\alpha(Q) = D - 3$. These two predictions cross the FPV prediction at $D = 10$ for $Q = 0$ and at $D = 5$ for $Q \neq 0$. It is unclear if something special happens at these two dimensions.

IV. METHODS

A. Direct measurement of the Interface Energy

We performed Monte Carlo simulations of the Edwards-Anderson model with binary couplings, equation 2, on the cubic lattice of size L with periodic boundary condition for $L = 4, 6, 8, 10, 12, 14, 16, 20$ in $D = 3$ and $L = 4, 5, 6, 7, 8, 9, 10, 12$ in $D = 4$ by means of a single spin flip dynamics with the usual Metropolis algorithm and using Parallel Tempering [24] to improve decorrelation and convergence. The lowest temperatures simulated in the Parallel Tempering protocol are $T = 0.7 \simeq 0.64T_c$ for $D = 3$ and $T = 1.4 \simeq 0.7T_c$ for $D = 4$ which are also the temperatures for which we show data in this work. We simulated $N_J = 12800$ different instances of the system.

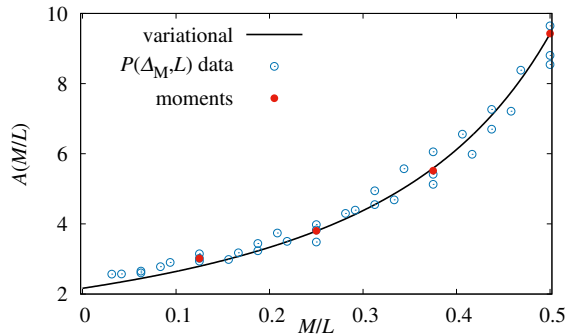


FIG. 3: The coefficient $A_{M,L}$ in the energy barrier (see equations 14, 15), obtained by i) fitting Monte Carlo $P(\Delta_M; L)$ data (open circles) with $M = 1, \dots, L/2$ and $L = 16, 24, 32$; ii) fitting the formula equation 15 to the second moment $\langle \Delta^2 \rangle$ (bullets) at ratios $M/L = 1/8, 1/4, 3/8$ and $1/2$; iii) variational computation in the continuum limit - see appendix C (continuous line). An overall factor to the variational data has been adjusted to match moments data (see text).

The simulation protocol we used to measure the interface barrier in the large Δ , $Q = 0$ sector is the following:

1. We thermalize a given instance of the system S ;
2. Once equilibrium is reached, the system is replicated twice: the replica $S^{(+)}$ retains periodic boundary condition; let's label site coordinates as $i = i_1, \dots, i_D$ in D dimensions; we apply antiperiodic boundary conditions in the D -th direction to the replica $S^{(-)}$;
3. We freeze spins on the $i_D = 0$ (hyper-)plane on both $S^{(+)}$ and $S^{(-)}$ (we inhibit their update in the single spin flip dynamics);
4. We thermalize both $S^{(+)}$ and $S^{(-)}$ and compute $\Delta E = \langle E(S^{(-)}) - E(S^{(+)}) \rangle$ where $\langle \dots \rangle$ is a thermal (Monte Carlo) average.
5. We repeat and collect statistics of ΔE over N_J samples.

If we compute overlaps between $S^{(+)}$ and $S^{(-)}$ on planes at fixed i_D

$$q(x) = \frac{1}{L^{D-1}} \sum_{i_1, \dots, i_{D-1}} \sigma_{i_D=x}^{(-)} \sigma_{i_D=x}^{(+)}, \quad (12)$$

in the limit of large L , $\Delta = |q(x=0) - q(x=L-1)|$ tends to the maximum allowed value, while $L^{-1} \sum_x q(x) \rightarrow 0$.

A related approach has been followed before in [25] to study the scaling properties of the interface energy in a different setting and with smaller system sizes, obtaining compatible results.

B. Large deviations of the overlap fluctuations

To extract data for the distribution $P(\Delta_M, L)$ we took profit of the Janus Collaboration's database [19, 20]. The dataset consists of many equilibrium configurations at different temperatures (in the number of $O(100)$ independent spin configurations per sample and per temperature

at the largest size) of 4000 samples of size $L = 16, 24$ and 1000 samples of size $L = 32$ of the $D = 3$ Edwards-Anderson model with binary couplings.

For each pair of spin configurations $\{\sigma\}$ and $\{\sigma'\}$ we compute the overlaps in boxes of size ML^2 :

$$q_M(z) = \frac{1}{ML^2} \sum_{z \leq i_D \leq z+M-1} \sigma_i \sigma'_i, \quad (13)$$

for $M = 1, \dots, L/2$ and collect statistics for $\Delta_M = \frac{1}{2}|q_M(z) - q_M(z + L/2)|$ in the sector $Q_M = \frac{1}{2}|q_M(z) + q_M(z + L/2)| < 1/16$ (this is an arbitrary cut-off chosen to soften the $Q_M = 0$ constraint enough to have satisfactory statistics; other $1/2$ factors are chosen to normalize Q_M and Δ_M in $[0, 1]$). The FPV prediction for the distribution of Δ_M is

$$P(\Delta_M, L) \propto \exp \left[-A_{M,L} L^{1/2} \Delta_M^{5/2} \right], \quad (14)$$

where the constant $A_{M,L}$ depends on the definition of the overlap, mainly on the boxes geometry through the ratio M/L . The moments of the distribution in equation 14 are combinations of Euler's gamma functions:

$$\langle \Delta_M^k \rangle = A_{M,L}^{2k/5} L^{-k/5} \frac{\Gamma((2k+2)/5)}{\Gamma(2/5)}, \quad (15)$$

and cumulants such as those in equation 11, should not depend on either A or L . For large L the coefficients $A_{M,L}$ should not depend on L as long as M/L is kept fixed. We estimate values of A from our data in two ways: i) by fitting equation 14 to $P(\Delta_M, L)$ data; ii) by fitting equation 15 to L dependent data at fixed M/L . Results are shown in figure 3. The extracted values compare well to estimates obtained in independent computations in the continuum limit (see appendix C), which are represented in figure 3 as a continuous line.

Acknowledgments

This project has received funding from the European Research Council (ERC) under the European Unions Horizon 2020 programme (grant No.694925). We thank S. Franz, who stimulated us in checking the FPV predictions on the scaling exponents, V. Astuti for very useful discussions on $\Delta F(L, \Delta)$, and the Janus collaboration for letting us analyze Janus data.

-
- [1] Wilson K G (1971) Renormalization Group and Critical Phenomena. I. Renormalization Group and the Kadanoff Scaling Picture *Phys. Rev. B* 4:3174; Wilson K G (1971) Renormalization Group and Critical Phenomena. II. Phase-Space Cell Analysis of Critical Behavior. *Phys. Rev. B* 4:3184; Wilson K G, Fisher M. E. (1972) Critical Exponents in 3.99 Dimensions. *Phys. Rev. Lett.* 28:240.
 - [2] Polyakov A M (1975) Interaction of goldstone particles in two dimensions. Applications to ferromagnets and massive Yang-Mills fields. *Phys. Lett. B* 59, 79; Migdal A A (1975) Phase transitions in gauge and spin-lattice systems. *Zh. Eksp. Teor. Fiz.* 69:1457; Brezin E, Zinn-Justin J (1976) Spontaneous breakdown of continuous symmetries near two dimensions. *Phys. Rev. B* 14:3110; Nelson D R and Pelcovits R A (1977) Momentum-shell recursion relations, anisotropic spins, and liquid crystals in $2 + \epsilon$ dimensions *Phys. Rev. B* 16, 2191.
 - [3] Franz S, Parisi G, Virasoro M-A (1994) Interfaces and lower critical dimension in a spin glass model. *J. Phys. I France* 4:1657.
 - [4] Mermin, N.D., Wagner, H. (1966) Absence of Ferromagnetism or Antiferromagnetism in One- or Two-Dimensional Isotropic Heisenberg Models. *Phys. Rev. Lett.* 17:1133.
 - [5] P. C. Hohenberg (1967) Existence of Long-Range Order in One and Two Dimensions. *Physical Review* 158:383.
 - [6] Edwards S F, Anderson P W (1975) Theory of spin glasses. *J. Phys. F: Metal Phys.* 5:965.
 - [7] Jing-Huei Chen, Lubensky T (1977) Mean field and ϵ -expansion study of spin glasses. *Phys. Rev. B* 16:2106;
 - Pytte E, Rudnick J (1979) Scaling, equation of state, and the instability of the spin-glass phase. *Phys. Rev. B* 19:3603.
 - [8] Harris A, Lubensky T, Jing-Huei Chen (1976) Critical Properties of Spin-Glasses. *Phys. Rev. Lett.* 36:415.
 - [9] Green J E (1985) ϵ -expansion for the critical exponents of a vector spin glass. *J. Phys. A: Math. Gen.* 18:L43.
 - [10] Gunnarsson K, Svedlindh P, Nordblad P, Lundgren L, Aruga H, Ito A (1991) Static scaling in a short-range Ising spin glass. *Phys. Rev. B* 43:8199
 - [11] Palassini M, Caracciolo S (1999) Universal Finite-Size Scaling Functions in the 3D Ising Spin Glass. *Phys. Rev. Lett.* 82:5128; Ballesteros H G et al. (2000) Critical Behavior of the Three-Dimensional Ising Spin Glass. *Phys. Rev. B* 62:14237.
 - [12] Boettcher S (2004) Stiffness exponents for lattice spin glasses in dimensions $d = 3, \dots, 6$. *Europ. Phys. J. B* 38:83.
 - [13] Boettcher S (2004) Low-temperature excitations of dilute lattice spin glasses. *Europhys. Lett.* 67:453.
 - [14] Boettcher S (2005) Stiffness of the Edwards-Anderson Model in all Dimensions. *Phys. Rev. Lett.* 95:197205.
 - [15] Fisher D S and Huse D A (1988) Equilibrium behavior of the spin-glass ordered phase. *Phys. Rev. B* 38:386.
 - [16] Baity-Jesi M et al. (2013) Critical parameters of the three-dimensional Ising spin glass. *Phys. Rev. B* 88:224416.
 - [17] Baños R A, Fernandez L A, Martin-Mayor V, Young A P (2012) Correspondence between long-range and short-range spin glasses. *Phys. Rev. B* 86:134416; Marinari

- E, Zuliani F (1999) Numerical simulations of the four-dimensional Edwards-Anderson spin glass with binary couplings *J. Phys. A: Math. Gen.* 32:7447; Jörg T, Katzgraber HG (2008) Universality and universal finite-size scaling functions in four-dimensional Ising spin glasses. *Phys. Rev. B* 77:214426.
- [18] Hartmann A K (1999) Scaling of stiffness energy for three-dimensional $\pm J$ Ising spin glasses. *Phys. Rev. E* 59:84; Hartmann A K (1999) Calculation of ground states of four-dimensional $\pm J$ Ising spin glasses. *Phys. Rev. E* 60:5135.
- [19] Baños R A et al. (2010) Nature of the spin-glass phase at experimental length scales. *J. Stat. Mech.* 2010:P06026
- [20] Baity-Jesi M et al. (2014) Janus II: a new generation application-driven computer for spin-system simulations. *Comput. Phys. Comm.* 185:550; Belletti F et al. (2008) Simulating spin systems on IANUS, an FPGA-based computer. *Comput. Phys. Comm.* 178:208.
- [21] Franz S, Jörg T, Parisi G (2009) Overlap interfaces in hierarchical spin-glass models. *J. Stat. Mech.* 2009:P02002.
- [22] Belletti F et al. (2009) An In-Depth View of the Microscopic Dynamics of Ising Spin Glasses at Fixed Temperature. *J. Stat. Phys.* 135:1121.
- [23] De Dominicis C, Kondor I, Temesvari T (1998) Beyond the Sherrington-Kirkpatrick model. *Spin Glasses and Random Fields* ed Young A P (World Scientific, Singapore) pp.119-160.
- [24] Geyer C J (1991) Markov Chain Monte Carlo Maximum Likelihood. Computing Science and Statistics, Proceedings of the 23rd Symposium on the Interface pp. 156-163; Hukushima K, Nemoto K (1996) Exchange Monte Carlo Method and Application to Spin Glass Simulations. *J. Phys. Soc. Japan* 65:1604; Marinari E (1998) Optimized monte carlo methods. *Advances in Computer Simulation* eds Kerstész J, Kondor I (Springer, Berlin) pp. 50-81.
- [25] Contucci P, Giardinà C, Giberti C, Parisi G, Vernia C (2011) Interface Energy in the Edwards-Anderson Model. *J. Stat. Phys.* 142:1.
- [26] Dobrushin R L, Shlosman S B (1975) Absence of breakdown of continuous symmetry in two-dimensional models of statistical physics. *Communications in Mathematical Physics* 42:31.
- [27] Parisi G (1988) *Statistical Field Theory* (Addison-Wesley, Boston) nsions. *Physical Review* 158:383.
- [28] Parisi G (1979) *Phys. Rev. Lett.* 43:1754; (1980) *J. Phys. A: Math. Gen.*13:1101; (1983) *Phys. Rev. Lett.* 50:1946.
- [29] Mézard M, Parisi G, Virasoro M (1987) *Spin-Glass Theory and Beyond* (World Scientific, Singapore).
- [30] Talagrand M (2006) The Parisi Formula. *Ann. of Math.* 163:221.
- [31] Sherrington D, Kirkpatrick S (1975) Solvable Model of a Spin-Glass. *Phys. Rev. Lett.* 35:1792.
- [32] Bricmont J, El Mellouki A, Fröhlich J (1986) Random surfaces in statistical mechanics: Roughening, rounding, wetting,... . *J. Stat. Phys.* 42:743; Lebowitz J L, Maes C (1987) The effect of an external field on an interface, entropic repulsion. *J. Stat. Phys.* 46:39.
- [33] The Janus Collaboration (2010) Static versus Dynamic Heterogeneities in the $D = 3$ Edwards-Anderson-Ising Spin Glass. *Phys. Rev. Lett.* 105:177202.
- [34] Wang W, Moore M A, Katzgraber H G (2017) Fractal Dimension of Interfaces in Edwards-Anderson and Long-range Ising Spin Glasses: Determining the Applicability of Different Theoretical Descriptions. *Phys. Rev. Lett.* 119:100602.
- [35] Marinari E, Parisi G (2000) Effects of changing the boundary conditions on the ground state of Ising spin glasses. *Phys. Rev. B* 62:11677.
- [36] An explicit computation shows that both the internal energy and the entropy increase have a similar behavior to the one of the free energy.
- [37] A less quantitative prediction comes from the value of the exponent η as a function of the dimensions D . This exponent strongly decreases when going from dimensions 4 to dimensions 3 where its value is $\eta(3) = -0.39 \pm 0.1$ [16]. We expect that at the critical dimensions $D_{lc} = 2 - \eta(D_{lc})$. A simple extrapolation of $\eta(D)$ would give $D_{lc} \approx 2.6$ with large errors. If we assume that $\eta(D)$ is a decreasing function of D (as it happens in all the extrapolations) the three-dimensional value implies that $D_{lc} > 2.4$.
- [38] We expect that the upper and the lower critical dimensions are simple rational numbers in the rare case that they are not integers (non-integer values are possible: for example the upper critical dimension for a quadricritical point - that is represented by a ϕ^8 interaction - is $8/3$).
- [39] It was assumed that we have a Landau-Ginsburg type functional whose form is obtained neglecting loop corrections to mean field theory.
- [40] We keep the quadratic terms in θ in the free energy or equivalently the linear ones in the mean-field equations.

Appendix A: Barriers in the Heisenberg ferromagnet

Let us see how to do such a computation in the Heisenberg ferromagnet: the spins are unit vectors on a three-dimensional sphere [26, 27]. We consider a D dimensional system, with periodic conditions in all directions x_2, \dots, x_D , but in the $x_1 \equiv x$ direction where we impose fixed boundary conditions. In the plane $x = 0$ and $x = L - 1$ we set respectively $\sigma = \{1, 0, 0\}$ and $\sigma = \{\cos(\theta_B), \sin(\theta_B), 0\}$. Our aim is to compute the ground state energy as a function of L and θ_B . For convenience, we consider only the variation $\Delta E(\theta_B, L)$ of the energy with respect to the ground state energy with periodic boundary conditions.

To this end we can consider only spins of the form $\sigma(\vec{x}) = \{\cos(\theta(\vec{x})), \sin(\theta(\vec{x})), 0\}$. In the limit of large L the space dependent phase $\theta(\vec{x})$ is a smooth function; neglecting lattice effects we can write

$$\Delta E(\theta_B, L) = A \int_0^L dx^D \sum_{\nu=1, D} \left(\frac{\partial \theta(\vec{x})}{\partial x_\nu} \right)^2, \quad (\text{A1})$$

where A is a positive constant.

Translational invariance is explicitly broken by the boundary conditions only in the x direction, so it is safe to assume that $\theta(\vec{x})$ is a function of only $x_1 \equiv x$. We thus arrive to

$$\Delta E(\theta_B, L) = AL^{D-1} \int_0^L dx \left(\frac{d\theta(x)}{dx} \right)^2. \quad (\text{A2})$$

If $\theta_B = 0$, i.e. periodic boundary conditions, the ground state is obviously given by $\theta(x) = 0$: $\Delta E(0, L) =$

0. If $\theta_B \neq 0$, the energy minimum is given by a smooth interface $\theta(x) = \theta_B x/L$. The energy increase is $AL^{D-2}\theta_B^2$, hence $D_{lc} = 2$. Indeed in $D = 2$ the energy difference remains of order 1, also when $L \rightarrow \infty$. Showing that the same argument can be used also at non zero temperature to prove the nonexistence of ordered phases requires a more complex proof.

The proof of the Mermin-Wagner-Hohenberg theorem [4, 5] about the absence of a phase with non-zero order parameter in two dimensional systems is quite different from the one presented here. In the MWH proof, one considers small fluctuations around equilibrium, here one considers large deviations from equilibrium, however, the physics foundations are the same.

If we extend this computation to the free energy at finite temperature, we obtain similar results, and the same method can be used to study the behavior of the correlations functions. We can get the final result in a fast way if we use dimensional analysis. Indeed, with an appropriate rescaling, we can set $A = 1$ and the combination $L^{D-2}\theta_B^2$ becomes dimensionless. If we assign to the length dimension -1, $\theta(x)$ must have dimensions $(D-2)/2$. Dimensional counting implies then that the correlation $C(x) \equiv \langle \theta(x)\theta(0) \rangle$ decays as $|x|^{-\alpha}$ with $\alpha = D-2$. The same formula in momentum space reads as $\tilde{C}(k) \propto 1/k^2$, that is what we expect from the Goldstone model.

Appendix B: The definition of the order parameter in mean field theory

The construction of the order parameter is quite complex [28, 29]: we consider an infinite number of equilibrium configurations $\{\sigma^\alpha\}$, with $\alpha = 1, \dots, \infty$. We can compute the overlaps $q^{\alpha, \gamma} \equiv \frac{1}{L^D} \sum_i \sigma_i^\alpha \sigma_i^\gamma$. Let us denote by \mathcal{Q} this infinite matrix. The probability distribution of the values Q in the overlap matrix \mathcal{Q} defines a function $P_J(Q)$ which changes with the disorder configuration $\{J\}$. Denoting by $[\dots]_J$ the average over different instances, we finally define $\bar{P}(Q) = [P_J(Q)]_J$ as the average over $\{J\}$ of $P_J(Q)$. The function $\bar{P}(Q)$ is the order parameter of spin glasses in the mean field limit. Indeed it is possible to construct a functional free energy $F[\bar{P}]$ such that in the mean field limit one can obtain the equilibrium value of the free energy by a variational principle. All this has been rigorously proven [30] in the Sherrington-Kirkpatrick [31] model where the mean field theory was supposed to be correct.

Appendix C: The computation of the free energy barrier as function of M/L

Let's consider a model as simple as a chain of L continuous variables q_i with periodic boundary conditions, for which we write the analogous of the free energy cost

(see eq. 6) as

$$\Delta F[q] = \sum_i |q_i - q_{i+1}|^{5/2} - \sum' q_i + \sum'' q_i, \quad (\text{C1})$$

where the second and third terms are sums over two regions of $M \leq L/2$ consecutive sites, taken at the largest possible distance $L/2 - M$. We may take \sum' in the region $0 \leq i < M/2$, $L - M/2 \leq i < L$, and \sum'' in the region $L/2 - M/2 \leq i < L/2 + M/2$. Such terms favor configurations with opposite total overlaps in the two regions of size M . We can numerically minimize the action above for any given M , finding an optimum q_i^o and computing $\Delta_M = (1/M) |\sum' q_i^o| = (1/M) |\sum'' q_i^o|$ and then the quotients $A_{M,L} = \Delta F[q^o]/\Delta_M^{5/2}$ as functions of M and L

We can also do an analytic computation directly in the continuum limit considering the functional:

$$\Delta F[\partial_x q(x)] = \int_0^1 dx \left| \frac{\partial q(x)}{\partial x} \right|^{5/2}, \quad (\text{C2})$$

with $q(x)$ a function in $[0, 1]$ with the following constraints and symmetries: we impose $q(0) = q(1) = q(1/2) = 0$, $q(x) = -q(1-x)$, $q(x) = q(1/2-x)$ for $x < 1/2$ and then $q(1/4) = Q_0$, $q(3/4) = -Q_0$ with, say, $Q_0 > 0$. We consider the variational problem with the constraint that the sum of the total overlaps in two regions of size z , one centered in $x = 1/4$ and the other in $x = 3/4$, with $0 < z < 1/2$, must be zero:

$$\Delta F_\lambda[q, \partial_x q(x)] = \int_0^1 dx \left| \frac{\partial q(x)}{\partial x} \right|^{5/2} - \lambda \left[\int_{\frac{1}{4}-\frac{z}{2}}^{\frac{1}{4}+\frac{z}{2}} dx q(x) + \int_{\frac{3}{4}-\frac{z}{2}}^{\frac{3}{4}+\frac{z}{2}} dx q(x) \right], \quad (\text{C3})$$

Given the symmetries, the extremum and the dependence of the multiplier λ on z are obtained requiring regularity of the extremal function $q(x; \lambda)$ and its derivative in $x = 1/4$ and $x = 1/4 - z$. The expression derived for $q(x; \lambda)$ is used for computing the free energy cost $\Delta F[q(x; \lambda)]$ (equation C2), the overlap fluctuation $\Delta(z) = (2/z) \int_{1/4-z/2}^{1/4} q(x; \lambda)$ and, up to an overall factor, the ratio $A(z) = \Delta F/\Delta(z)^{5/2}$ as a function of z , which plays the role of M/L above.

The two computations give similar results. Figure 3 shows the results of the analytic computation in the continuum limit compared to the coefficients $A_{M,L}$ appearing in equation 14, and obtained by analyzing Monte Carlo data. As one can see, barring renormalization constants, values of $A_{M/L}/A_{M'/L}$ obtained from Monte Carlo data compares well to estimates by these two methods.

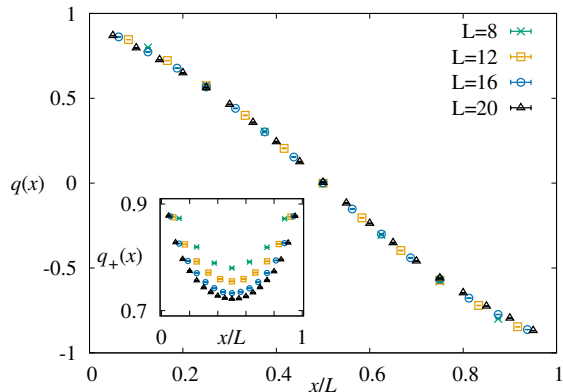


FIG. 4: The overlap $q(x)$ between the S^+ (PBC) and S^- systems (see section *Methods*, equation 12, and the appendix D), as a function of x/L . In the inset, the overlap q_+ between S^+ and the reference configuration of the non-constrained system, from which S^+ and S^- have been replicated, as a function of x/L .

Appendix D: Comparison to previous estimates of the stiffness exponent

The overlap protocol used in the simulations here yields a different scaling from domain-wall stiffness exponent considered in [12–14, 18], although both analyses agree on the value of the lower critical dimension. Let us summarize the main different features of the protocol:

1. Our approach involves a thermal and a disorder average at finite temperature instead of the pure disorder average at $T = 0$ in [12–14, 18].
2. We go from periodic to antiperiodic boundary conditions as in [12–14, 18]. However, we add the further constraint that the spins of a hyperplane remain fixed.

We believe that condition (2) makes the main difference while (1) is a just a technical difference: however it would be extremely interesting to check numerically what happens a $T = 0$ on the same samples following both protocols.

The previous investigations [12–14, 18] on scaling with size of domain-wall energy in the EA model (equation 2) considered energy differences ΔE_J of ground states of a spin glass sample (a given disorder configuration) upon changing from periodic (PBC) to antiperiodic boundary conditions (APBC) in one direction.

In ground state computations, random interfaces induced by the change in boundary conditions adjust to and take advantage of bond frustration to minimize their energy. Given the random disorder, the sample average of the energy differences ΔE_J between PBC and APBC vanishes. The relevant quantity is the absolute value $|\Delta E_J|$; on the contrary in our case the energy variation is always positive definite. One expects for the sample

average of the magnitude of the difference to scale as $[|\Delta E_J|]_J \sim L^{\mathcal{Y}_D}$ with the *stiffness* exponent $\mathcal{Y}_D > 0$ at dimensions above D_{lca} and $\mathcal{Y}_{D_{lca}} = 0$. The estimates [13] for the D dependent stiffness exponent are $\mathcal{Y}_{D=3} \simeq 0.24$ and $\mathcal{Y}_{D=4} \simeq 0.61$, which are well below the estimates for interface energy exponents in the present work (our exponents are roughly speaking a factor two larger). Of course, we are studying our systems at finite temperature, and we cannot exclude a dependence on T of the stiffness exponent, but we are actually considering the scaling properties of quantities which are distinct from (albeit probably non-trivially related to) the ones considered in ground state studies.

In order to test the FPV prediction (equation 8) we need to constrain two independent replicas S^+ and S^- for a given sample as described in the *Methods* section. The two replicas have a given total mutual overlap fluctuating around $Q = 0$ (in our specific case) and the maximum possible overlap difference along one direction $\Delta = |q(x=0) - q(x=L-1)|$, where $q(x)$ (see equation 12) is the overlap on the plane orthogonal to the x direction and of given x coordinate. Freezing all spins on the $x = 0$ plane (to values of an equilibrium configuration of the original system) on both replicas ($q(x=0) = 1$) and imposing APBC along the x axis on S^- are the device by means of which we impose the constraint. The frozen spins act as an external field breaking the underlying symmetries and favoring configurations with large positive mutual overlap in the system S^+ which retains periodic boundary conditions. In S^- , with APBC, an interface develops as a result of the energy cost introduced by flipping the boundary. Since the spins on the border are frozen and drive the system towards configurations strongly correlated to the equilibrium configuration of S^+ , the configuration of spins in S^- is not free to relax toward an equilibrium state which would be typical of its disorder configuration (factoring in APBC), resulting in a positive average energy difference ΔE at the interface between two spin-reversed phases, as in the case of the Ising ferromagnet.

In addition, given the frozen configuration on the $x = 0$ plane, the interface cannot cross the boundary without additional free energy cost; entropic repulsion pushes it towards the central region (it moves away from the wall in the search of space to fluctuate) [32]. As a result, the induced interface is not as free to adjust to frustrated links as in the standard ground state computations, giving rise to a different definition of the scaling exponent.

The situation would be analogous, although more complicated, in the general case, say, $Q > 0$ and $\Delta < 2 - 2Q$ which is harder to implement in a direct simulation. In that case the interface would result from the competition of two phases with overlaps $Q - \Delta$ and $Q + \Delta$ at opposite borders, not related by any simple symmetry.

We show the overlap $q(x)$, equation 12, between systems $S^{(+)}$ and $S^{(-)}$ as a function of x/L in figure 4 for $D = 3$, $T = 0.7$, in our case of study: $Q > 0$ and $\Delta = 2$. This scaling shows that we are not

far from the asymptotic limit. In the same figure we also show, as a function of x/L , the overlap $q_+(x) = \frac{1}{L^{D-1}} \sum_{i_1, \dots, i_{D-1}} \sigma_{i_D=x}^{(\text{ref})} \sigma_{i_D=x}^{(+)}$, where $\{\sigma^{(\text{ref})}\}$ is the equilibrium spin configuration of the original system from which S^+ and S^- are replicated (see section *Methods*). $q_+(x)$ takes large values for all x , well above the value of $q_{EA}(T=0.7) \simeq 0.52$. [19, 33]

We have observed that in the case of PBC-APBC, the energy difference ΔE has a random sign: the average of ΔE is zero and the interesting observable is the average of $|\Delta E|$. In our case the energy variation ΔE has a non zero average; in three and four dimensions this average is asymptotically larger than the average of $|\Delta E|$ with the other protocol (the exponent is nearly a factor two larger).

We would like to further speculate on the possible physical origins of this difference. Let us discuss what happens in the PBC-APBC protocol. Changing the boundary condition at $T=0$ introduces a relative interface plane between spins that are flipped and the spins that are not flipped. A crucial point is the fractal dimensions of this interface. Two different scenarios are possible

- In the large volume limit, this interface is essentially localized around a plane dividing the system into two regions: a region where the new ground state is equal to the original ground state and a region where the new ground state is the spin reversed one. The interface could be rough, but as

far as its fractal dimension d_F is less than the space dimensions D the value of d_F is irrelevant. In this scenario, the interface of our work should behave in a way quite similar to the interface of PBC-APBC. Indeed, for large volume, the interface we create should be able to avoid the parallel plane of fixed spins, since its location along the D -direction is arbitrary. In this scenario, the energetics of this protocol should be the same of PBC-APBC.

- In an alternative scenario in the large volume limit this interface is not localized in a particular region and it is space filling ($d_F = D$). There are no large regions where the new ground state is similar to the old ground state. In this scenario, if we force the system in a given region to be similar to the original one, we have to pay an additional energy cost and this explains the difference between the two protocols.

The first scenario has been advocated by Wang et al. [34] in the framework of an approximate computation of the ground state; the second scenario has been advocated by Marinari and Parisi [35] using information from exact ground states on systems of sizes up to 14^3 .

We think that it would be very interesting to use modern technologies to check which of those two scenarios is the correct one at $T=0$, also in order to clarify the origin of the difference of our exponents with those of [12–14, 18].